


Transcriptomic analysis reveals myometrial topologically associated domains linked to the onset of human term labour

Sonika Tyagi ¹, Eng-Cheng Chan², Daniel Barker³, Patrick McElduff³, Kelly A. Taylor², Carlos Riveros³, Esha Singh⁴, and Roger Smith ^{2,3,*}

¹Department of Infectious Diseases, Central Clinical School, Monash University and the Alfred Hospital, Melbourne, VIC, Australia ²Mothers and Babies Research Centre, HMRI University of Newcastle, NSW, Australia ³University of Newcastle, Newcastle, NSW, Australia ⁴Department of Biotechnology and Biochemical Engineering, Indian Institute of Technology, New Delhi, India

*Correspondence address. Endocrinology Department | Medical & Interventional Service, John Hunter Hospital, Lookout Road, New Lambton Heights, NSW 2305, Australia. E-mail: Roger.Smith@newcastle.edu.au  <https://orcid.org/0000-0003-4720-0280>

Submitted on October 05, 2021; resubmitted on January 10, 2022; editorial decision on February 03, 2022

ABSTRACT: Changes in cell phenotype are thought to occur through the expression of groups of co-regulated genes within topologically associated domains (TADs). In this paper, we allocate genes expressed within the myometrium of the human uterus during the onset of term labour into TADs. Transformation of the myometrial cells of the uterus into a contractile phenotype during term human labour is the result of a complex interaction of different epigenomic and genomic layers. Recent work suggests that the transcription factor (TF) RELA lies at the top of this regulatory network. Using deep RNA sequencing (RNAseq) analysis of myometrial samples ($n = 16$) obtained at term from women undergoing caesarean section prior to or after the onset of labour, we have identified evidence for how other gene expression regulatory elements interact with TFs in the labour phenotype transition. Gene set enrichment analysis of our RNAseq data identified three modules of enriched genes (M1, M2 and M3), which in gene ontology studies are linked to matrix degradation, smooth muscle and immune gene signatures, respectively. These genes were predominantly located within chromosomal TADs suggesting co-regulation of expression. Our transcriptomic analysis also identified significant differences in the expression of long non-coding RNAs (lncRNA), microRNAs (miRNA) and TFs that were predicted to target genes within the TADs. Additionally, network analysis revealed 15 new lncRNA (MCM3AP-ASI, TUG1, MIR29B2CHG, HCG18, LINC00963, KCNQ1OT1, NEAT1, HELLPAR, SNHG16, NUTM2B-ASI, MALAT1, PSM3-ASI, GABPBI-ASI, NORAD and NKILA) and 4 miRNA (*mir-145*, *mir-223*, *mir-let-7a* and *mir-132*) as top gene hubs with three TFs (NFKB1, RELA and ESRI) as master regulators. Together, these factors are likely to be involved in co-regulatory networks driving a myometrial transformation to generate an estrogen-sensitive phenotype. We conclude that lncRNA and miRNA targeting the estrogen receptor 1 and nuclear factor kappa B pathways play a key role in the initiation of human labour. For the first time, we perform an integrative analysis to present a multi-level genomic signature made of mRNA, non-coding RNA and TFs in the myometrium for spontaneous term labour.

Key words: pregnancy / estrogen / parturition / topologically associated domains / epigenome / bioinformatics

Introduction

Higher-order chromatin structure and organization is emerging as a key factor in determining how *cis*-regulatory elements work to generate a phenotype or disease risk (Lupiáñez *et al.*, 2015; Franke *et al.*, 2016; Merienne *et al.*, 2019; Liang *et al.*, 2020). Along the linear DNA axis, there are domains of DNA that tend to interact with each other more frequently than with areas outside the interacting domains: these

are termed topologically associated domains (TADs; Hou *et al.*, 2012; Nora *et al.*, 2012; Sexton *et al.*, 2012). Evolutionary conservation of TADs between species and cell types suggests their functional relevance (Dixon *et al.*, 2015). TADs are important features of genome organization not only to facilitate chromatin packing but also to restrict enhancer–promoter interactions to the TAD, and breaking of TAD boundaries has pathological consequences (Lupiáñez *et al.*, 2015; Merienne *et al.*, 2019). Recent work on the transformation of cell

phenotypes has emphasized the role of co-regulation of groups of genes within TADs to effect major changes in the structure and behaviour of cells (Phillips-Cremins et al., 2013). Higher resolution analysis of TADs has shown that TADs have hierarchical structures forming sub-TAD structures, also known as chromatin loops (Rao et al., 2014). Further, CTCF or CCCTC-binding factor is an evolutionary conserved and multifunctional protein that appears to have a role in insulating the TAD boundaries to constrain enhancer–promoter interactions within the domains (Narendra et al., 2015).

Successful human parturition requires the uterus to undergo a programme of transformation from a quiescent expandable receptacle into an active organ able to produce coordinated forceful phasic contractions to push the foetus through a softened cervix to birth (Smith et al., 2012, 2013, 2019, 2020; Kota et al., 2013; Smith, 2015). An understanding of the programme at the molecular level is central to developing precision obstetric interventions for at-risk pregnancies, including to stop premature delivery, successfully induce normal vaginal delivery or to promote uterine contraction to arrest post-partum haemorrhage (Smith et al., 2019). With practical and ethical constraints on experimental approaches and an absence of applicable animal models for human parturition, efforts to understand the programme have focused on mathematical modelling of key variables from single samples of human myometrium obtained at caesarean section.

We and others have interrogated genomic and transcriptomic data from term human myometrium to gain insight into the process of labour in parturition. Previously, several studies have employed gene expression profiling using microarray (Esplin et al., 2005; Bukowski et al., 2006; Mittal et al., 2010; Romero et al., 2014; Sharp et al., 2016; Lui et al., 2018) or high-throughput RNA sequencing (RNAseq) to identify genes that are differentially expressed during parturition (Ackerman et al., 2018; Stanfield et al., 2019). These studies have generated a long list of genes that are altered during the process of labour (Stanfield et al., 2019). Although myometrial contractility has been associated with a characteristic gene expression pattern, finding the key drivers from the long differentially expressed list is challenging. We postulated that an interaction of epigenomic factors, including non-coding RNA (ncRNA), and specific gene regulation control determines the transcriptional phenotype. We have examined the hierarchical architecture of the genomic components to identify likely apical drivers of large-scale transcriptional changes within specific TADs (Fig. 1).

Materials and methods

Ethics approval

The samples were collected under our University of Newcastle John Hunter Hospital, Newcastle, Australia and the Singapore KK Women's and Children's Hospital ethics committees (Ethics approval H3820602). Pregnant women gave written informed consent to donate a biopsy of their myometrium at caesarean section at term according to the institutional guidelines and regulations.

Patient recruitment and tissue sampling

Women undergoing elective caesarean section without uterine contractions formed the not-in-labour (N, n = 31) group. Women who

entered spontaneous and established labour for at least 2 h, but required emergency surgery, formed the term in-labour (L, n = 29) group. Following delivery, the placenta and membranes were examined for chorioamnionitis. Women displaying clinical or histological indications of infection were excluded from the study. Clinical indications for the emergency section L group included breech, macrosomia, foetal distress, failure to progress and low amniotic fluid index, while subjects in the N group underwent surgery owing to previous caesarean sections. All women were between 36 completed weeks and 40 weeks gestational age. Tissues were sampled using a surgical technique standardized such that the bladder is reflected off the lower segment of the uterus (the uterovesical-fold) and the uterine incision is made in the upper part of the lower segment. Connective tissue and decidua were removed, and the tissues snap frozen in liquid nitrogen and stored at -80°C until analysis.

The tissues were extracted by the guanidinium thiocyanate-acid phenol-chloroform method as described previously (Chan et al., 2002) and 21 genes experimentally found by the RNA subtraction method to be differentially up-regulated were analysed by Bioinformatics (Ingenuity Pathway Analysis) analyses and published data. Twelve genes identified from the post-subtraction *in silico* analyses were added to the earlier group of 21 genes for confirmation by quantitative RT-PCR, with only 29 of the 33 found to increase significantly with labour in a cohort separate from the subtraction study (Chan et al., 2002; Supplementary Table S1). Z-scores for each gene were calculated from the data of all 60 women, and the z-scores of the 29 mRNA species for each mother were combined to form her overall gene expression ranking in the study cohort. For each mother, a radar plot was generated including data for the 29 genes. Mothers were then ranked from 1 to 60 based on their mean z-score data (Supplementary Fig. S1a). The radar plots were combined to generate a cigar plot showing the transition from not-in-labour to in-labour status, which largely, but not completely, aligned with the clinical characterization of their status (Supplementary Fig. S1b). This is consistent with uncertainty over how close to labour and delivery each mother may be, as clinical characterization is notoriously difficult for both the woman and her clinician (Romero et al., 2006; Hanley et al., 2016), while the cervical changes used to diagnose the mother's labour status can be misleading since many patients with cervical shortening show no clinical signs of uterine contractions (Myers et al., 2015). We propose that the ranking order represents a surrogate for time that indicates the position of the mother on the pathway to labour and delivery. Candidates for whole transcriptome analysis using RNAseq were chosen from the two distal ends of the cigar plot (Supplementary Fig. S1b, i.e. non-labouring (n = 6), and labouring (n = 6) groups as well as women clinically classified as labouring from the middle band to represent mothers in early labour (n = 5)).

RNA sequencing

Paired-end sequencing of 17 human whole RNA stranded samples was performed on an Illumina HiSeq 2500 platform at the Australian Genomics Research Facility Ltd. (AGRF). Sample integrity was checked on an Agilent Bioanalyzer and all samples had RNA integrity number >7 . Samples were first depleted of ribosomal RNA with Illumina Ribo-zero Gold. The rRNA-depleted samples were fragmented using heat and divalent cations before reverse transcription with SuperScript II kit

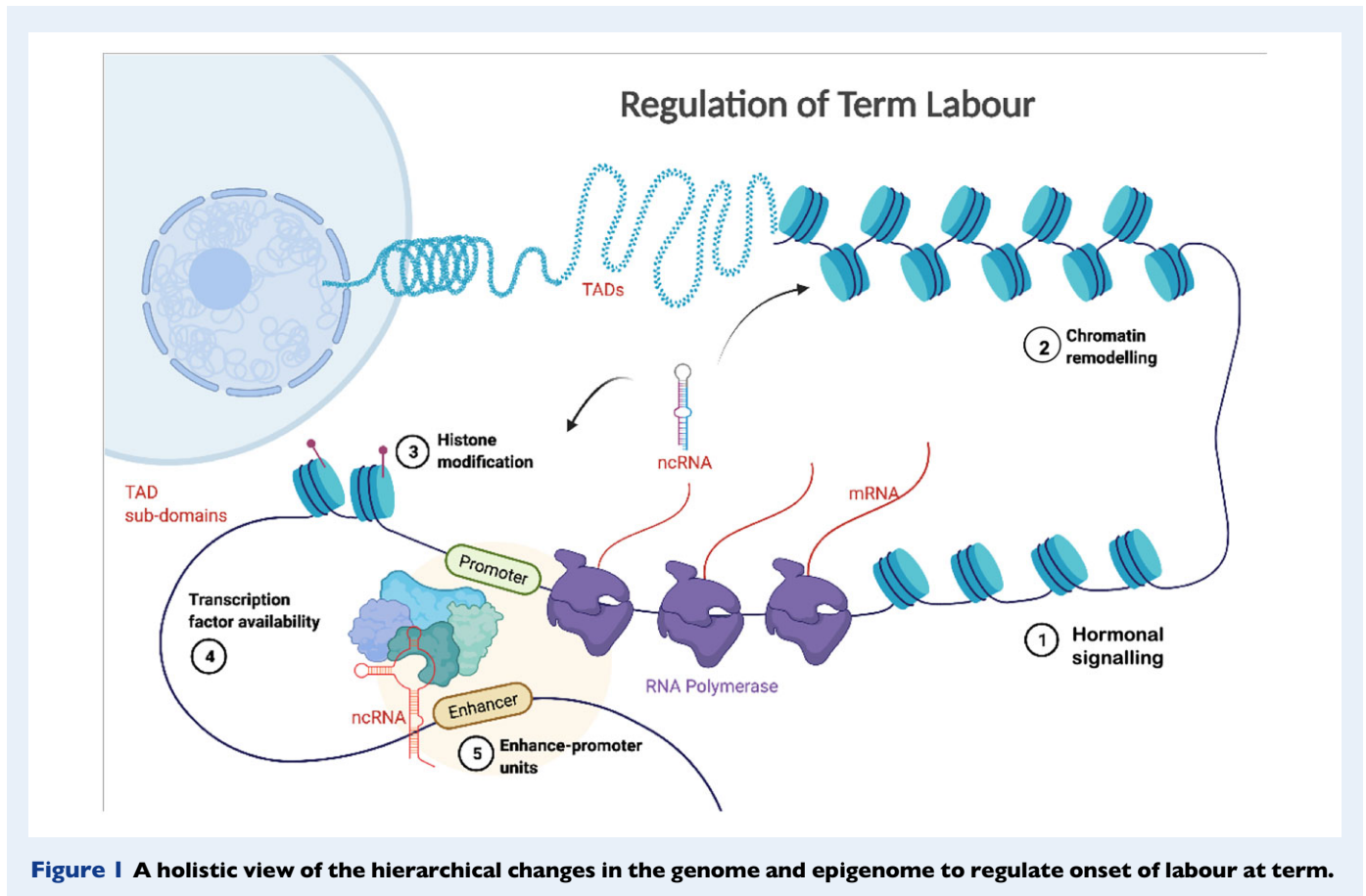


Figure 1 A holistic view of the hierarchical changes in the genome and epigenome to regulate onset of labour at term.

(Invitrogen). Ultra-deep sequencing was carried out generating 100–150 million usable reads per sample. The whole RNA content therefore includes both protein-coding and ncRNA transcripts.

Data analysis

RNAseq data analysis

Clean RNAseq reads were aligned to human genome build hg38 using the HISAT2 (Kim *et al.*, 2019) aligner. The aligned (.bam) files were then used to summarize counts for known protein-coding and non-coding gene annotations (GENCODE version 33) using the FeatureCounts utility of the Subread package (Liao *et al.*, 2019, 2014). During the quality control step, it was observed that non-labouring samples (except for EC1) clustered together but samples from the early and late labour group were not clearly separated in the hierarchical clustering (Supplementary Fig. S2a–c). Based on these observations, we first removed one sample (EC1) from the non-labouring group and the remaining 16 ($n = 5 + 5 + 6$) samples were further processed. Second, we identified a signature based on groups of protein-coding genes associated with each of the phenotypic groups (Supplementary Fig. S2d).

Coding-gene counts were used to identify ‘modules’ of co-expressed genes and generate gene expression signatures related to each sample within a phenotypic group (Zhang and Horvath, 2005). Thus, from the whole transcriptome data, we generated the gene expression signatures representative of each of the no-labour, early labour and late labour groups by considering co-expressed gene modules using an R-based tool called CEMiTool (Russo *et al.*, 2018).

Gene set enrichment analysis (GSEA) was performed for each module. GSEA associated activity of each module within each sample class was then represented as a net enrichment score, which corresponds to a shifting of gene set constituents of a module towards either end of a ranked list representing strongly positive or negative correlations. To associate biological function to each of the modules, we examined over-represented pathways in each co-expressed module.

From the reads, two classes of ncRNA profiles were also generated, these were long non-coding RNA (lncRNA) and microRNA (miRNA) using GENCODE (Frankish *et al.*, 2019) and miRBASE (Kozomara *et al.*, 2019) reference annotations, respectively. FeatureCount (Liao *et al.*, 2014) and EdgeR-Voom packages (Robinson *et al.*, 2010; Law *et al.*, 2014) were used to perform the gene expression analysis. The ncRNA counts vary in their abundance and additionally, a co-expression network analysis was not possible for a large number of ncRNA captured in our analysis. Therefore, for ncRNA expression analysis, we combined the two labouring groups ($n = 5 + 6$) into one and compared this single group against the non-labouring group ($n = 5$). Since miRNAs are known to repress expression of their target mRNAs and have inverse correlations with their target lncRNAs, we computed negative Pearson correlations between the miRNA:mRNA and miRNA:lncRNA. We summarized results for $\text{adj.pval} < 0.05$, and at different correlation cut-offs. As lncRNA is known to negatively regulate miRNAs, we confirmed known miRNA:lncRNA and gene:target pairs using databases such as Starbase (Yang *et al.*, 2011) and RNAInter (Lin *et al.*, 2020) that contain experimental data from multi-omics studies.

Using the overrepresentation analysis tool from the Reactome database (Reimand et al., 2019), we performed pathway enrichment analysis of differentially expressed miRNAs. This uses a hypergeometric distribution to test for significance and false discovery rate (FDR) to correct for multiple testing (Reimand et al., 2019). Gene set analysis of lncRNA was performed using the lncCompare database (Carlevaro-Fita et al., 2019), and genes miRNet2.0 (Chang et al., 2020) for miRNA.

Regulatory elements

The 3-dimensional structure of the genome and chromatin remodelling facilitates transcription, and the compartmentalization of transcriptional activities can be deduced by aggregating various types of genomic and epigenomic data. We have used this combined information to suggest causal relationships leading to an expression phenotype.

Topologically associated domains

Chromosomal looping can bring arrays of regulatory elements from distant parts of the genome to create high-level self-interacting contacts and form sub-mega base-pair TADs (Lieberman-Aiden et al., 2009; Bonev and Cavalli, 2016). Generally, TADs encompass interactions between enhancers and promoters, as well as between co-regulated genes, which reflect cell-type-restricted transcriptional programmes. Enhancers occur where arrays of permissive regulatory elements are grouped. TADs are surrounded by insulators at their boundaries, which prevent enhancers from exerting actions outside a domain (Zabidi et al., 2015). It has been shown that constitutively expressed genes, such as housekeeping genes, tend to be located at the boundaries of TADs (Dixon et al., 2012; Muro et al., 2019). Genes with more specialized roles tend to concentrate within a domain and may be under tighter gene regulatory control. We mapped genes from the three modules to their genome-wide contact domain locations (Rao et al., 2014).

Active enhancers

We investigated whether more than one of our genes of interest were located inside a TAD, and if they were sharing active enhancers. EnhancerAtlas 2.0 (Gao and Qian, 2020) was used to identify active enhancers associated with the genes that comprised the three identified gene modules. Next, we investigated the transcription factors (TFs) potentially involved in epigenome reprogramming for labour.

TF binding sites

To complete the regulatory complex view of the gene expression environment, we looked for TF binding sites (TFBS) both in the enhancer (EnhancerAtlas classification) and promoter (10 000 bp upstream and 5000 bp downstream of TSS) regions using a list of known TF motifs from the JASPAR database (Sandelin et al., 2004; Khan et al., 2018). In order to identify significantly enriched TFs, we subtracted the occurrence of these motifs by chance to obtain statistically enriched TFBS. The results were selected using an adjusted P -value < 0.05 cut-off (Kwon et al., 2012; Gearing et al., 2019).

Results

Gene expression signatures and cellular functions

The GSEA (Mootha et al., 2003; Subramanian et al., 2005) resulted in three significant modules represented as M1, M2 and M3 (Fig. 2) and

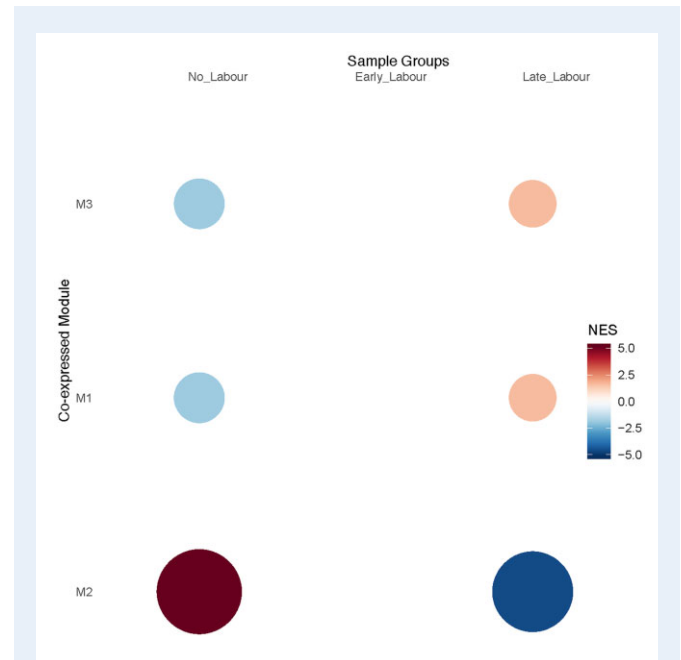


Figure 2 Gene set enrichment analysis for myometrium of the human uterus.

The net enrichment score (NES) for three samples groups are plotted on the x-axis; NL, no labour; EL, early labour and LL, late labour. The red colour represents higher activity and blue represents lower activity. The size of the circle is proportional to the NES scores. The average expression of the genes from the three modules is provided in Supplementary Table SII.

were composed of 81, 46 and 36 genes, respectively. We observed that M2 had higher expression in the no-labour stage (red), while expression of M1 and M3 was associated with the active labour state (Fig. 2). We did not observe a co-expressed gene module that can characterize the early labour stage; this may be due to high variance in this group relating to the intermediate state of the members of this group on the trajectory to labour.

The M1 module is enriched for pathways associated with matrix degradation (Fig. 3A), the M2 module exhibits a smooth muscle profile (Fig. 3B), and the M3 module shows enrichment for immune gene signatures (Fig. 3C). The size and strong positive correlation of the M2 module with the no labour state suggests the base-level expression signature of myometrium, and that these genes are associated with the maintenance of pregnancy. Some of these observations, such as the expression of cytokines and immune pathways in the M1 and M3 modules, are consistent with previous studies of the gene signatures of spontaneous term labour (Bethin et al., 2003; Keelan et al., 2003; Bukowski et al., 2006; Stanfield et al., 2019). Average expression of genes from the three modules is provided in Supplementary Table SII.

TADs may be related to co-regulation of gene expression

Mapping of our co-expressed gene modules to previously published genomic coordinates of TADs (Rao et al., 2014) was compared with that of randomly selected genes. We found that the genes from the three modules are non-randomly distributed (Kolmogorov–Smirnov

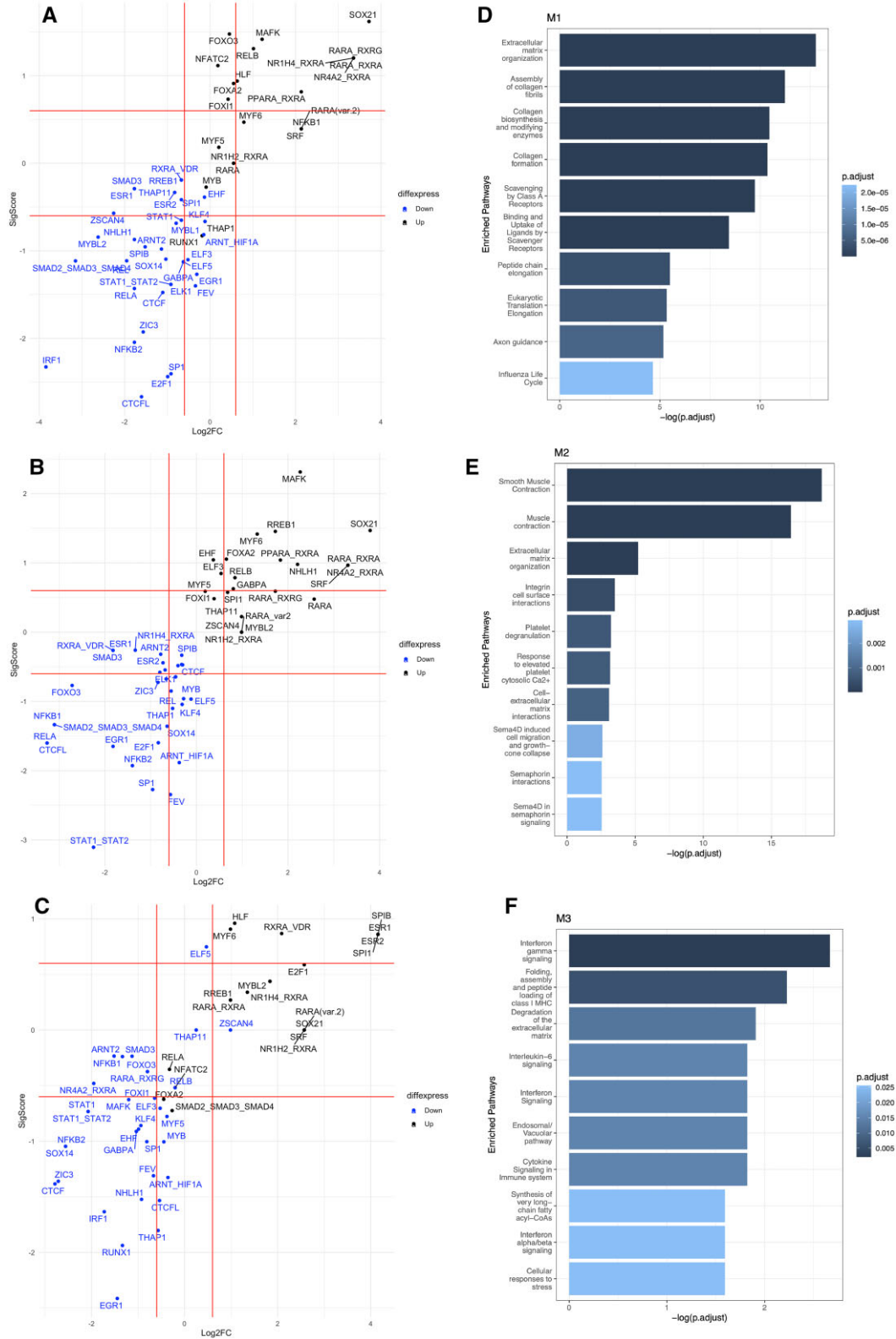


Figure 3 Active enhancers and pathways analysis for myometrium of the human uterus. The column on the left (A–C) shows transcription factor (TF) enrichment in the enhancers plotted as their log2 fold change between identified genes and the background sets versus the significance score computed as $-(\log_2FC) * \log_{10}(P\text{-value})$. TFs over- and under-represented for each of the three modules are shown in black and blue, respectively. The column on the right (D–F) shows pathway enrichment for genes in the modules M1, M2 and M3, respectively.

two-sided test P -value = 0.0006), with 76% of M2 genes, and 66% of both the M1, and M3 groups predominantly located within a topological domain as compared to randomly selected genes (Fig. 4). This suggests that the majority of the genes within the three co-expressed modules have specialized functions and are likely to be co-regulated. M1 genes at a TAD border are *COL1A2*, *IGFBP5*, *HSPA8*, *SPARCL1*, *COL5A1*, *ENO1*, *MACF1*, *GAPDH*, *CANX*, *VWF*, *FBLN1*, *UBC*, *HSP90AB1*, *RPL4*, *CSDE1*, *ALDOA*, *RACK1* and *RPS3*, which have roles in glycolysis, gluconeogenesis and amino acid biosynthetic pathways. Similarly, M2 genes at the border are *FLNA*, *MYH11*, *AHNAK*, *FLNC*, *CNN1* and *MAP1B*, which are involved in muscle fibre development and cell junction assembly. Finally, M3 genes at the border are *VCAN*, *MSN*, *MMP2*, *HLA-E*, *HLA-B*, *STAT3*, *VMPI1*, *RDH10* and *CXCL8*, which have roles in cytokine signalling and immune pathways.

TADs can be subdivided into subdomains that contain genes that have a higher likelihood of co-regulation. Enhancer–promoter interactions are required to form regulatory units and co-regulate genes in these subdomains. We mapped enhancer–promoter interactions onto our gene modules. These enhancer–promoter interactions are marked as red links in Fig. 5. Furthermore, analysis of TFBS in the promoter and enhancer regions revealed TFs that may regulate these genes, creating transcriptional units. We have demonstrated over- and under-represented TFs in the active enhancers for the three different gene modules (Fig. 6A–C). All three modules shared nine common TFs

(*NR1H2::RXRA*, *MYF6*, *RARA::RXRA*, *PPARA::RXRA*, *RARA(var.2)*, *FOXA2*, *SRF*, *RARA*, *SOX21*) in their enhancers. Five TFs were specific to M1 (*THAPI*, *NFKB1*, *MYB*, *FOXO3* and *RUNX1*), six TFs were specifically found in the enhancer regions of M2 (*EHF*, *NHLH1*, *ELF3*, *GABPA*, *THAPI1* and *ZSCAN4*) and 10 were M3 specific (*RXRA::VDR*, *ESR1*, *ESR2*, *SPIB*, *E2F1*, *ELK1*, *REL*, *MYBL1*, *RELA* and *SMAD2::SMAD3::SMAD4*). Overrepresented TFBS restricted to the promoter regions are summarized in Table 1 and as shown in Supplementary Fig. S3, the predictive scores of these TFBS are not affected by the genomic GC content.

ncRNA mediated regulation revealed by analysing gene expression profiles and target analysis

miRNA expression profiles

For profiling ncRNA expression, we merged the early and late labour groups and tested for differential expression between the no-labour and labour groups. The expression of 27 miRNAs changed significantly (FDR adjusted P -value ≤ 0.05) in the labour groups (Fig. 6A). The expression of 10 miRNAs decreased from the no-labour to the labour groups, whereas, 17 miRNAs increased their expression in the labour groups. More detailed annotations of these miRNA are available in Supplementary Table SIII.

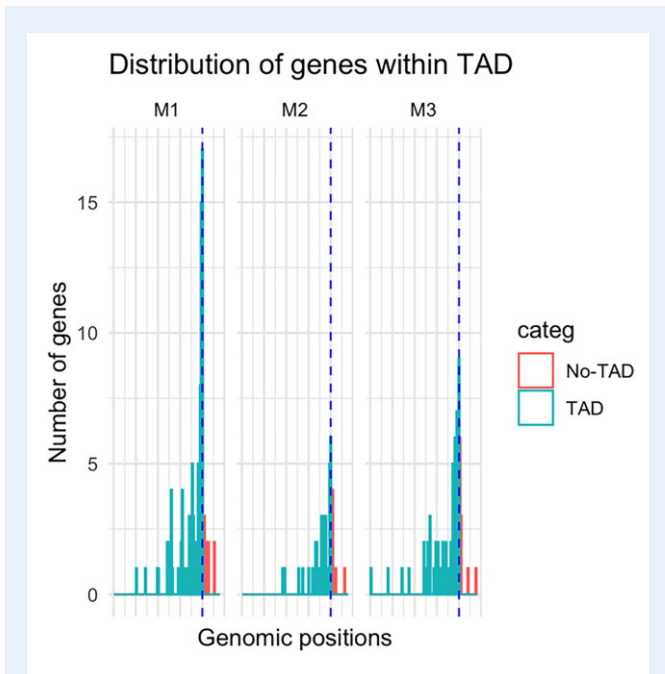


Figure 4 Distances of genes from modules M1, M2 and M3 calculated from the nearest known topologically associated domain (TAD) boundary. Here, the dashed blue line denotes the TAD boundary, the histogram of gene counts shows that the majority of the genes are inside known TADs and a small proportion lie near the boundary or outside the domain. As shown, 66% of M1 and M3 genes, and 76% of M2 genes lie within the TAD regions.

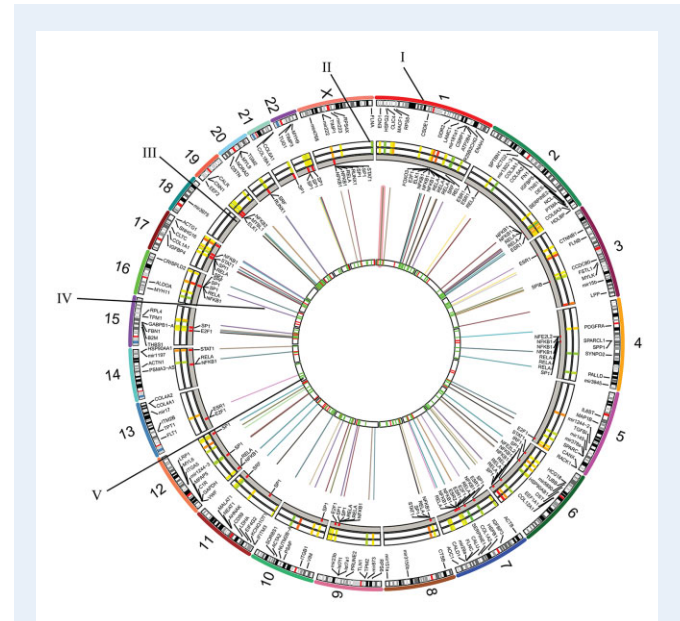
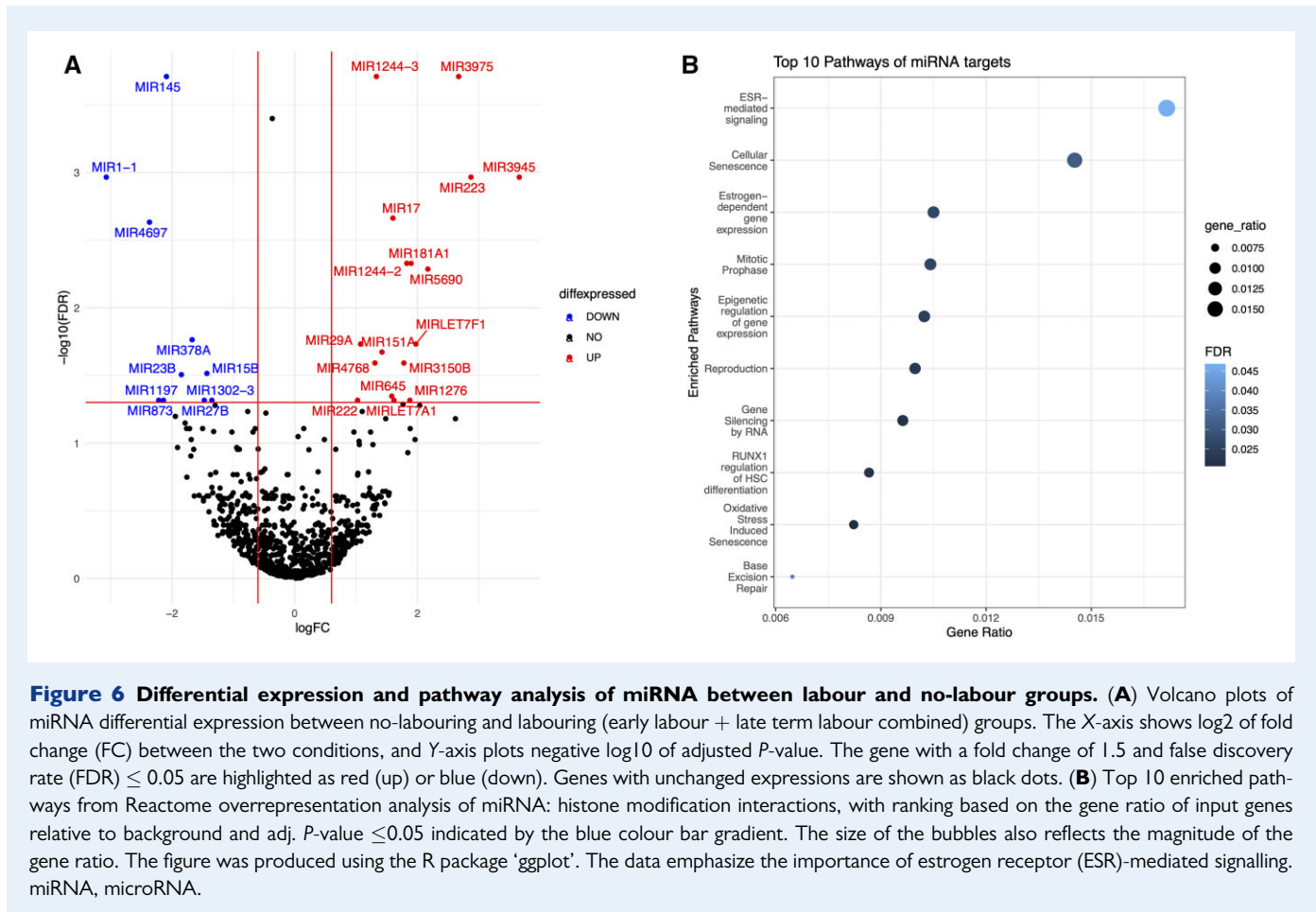


Figure 5 Map of genomic and epigenomic factors driving the human term labour phenotype. Outermost track (I) displays coding genes from the three identified modules, and non-coding genes (long non-coding RNA and microRNA: mir). Next, the gene expression heatmap (II) is plotted as up- (red) and down-regulated (yellow). This is followed by the transcription factor binding site track (III). Enhancer–promoter interactions are shown by multi-coloured lines (IV). The innermost circle (V) shows the TAD (green) or No-TAD (red) location of the genes in the outermost layer. TAD, topologically associated domain.



miRNA targets, namely mRNA and lncRNA, were identified and then analysed for their involvement in different biological pathways. As shown in Fig. 6B, a total of 25 enriched pathways (adj. P-value ≤ 0.05) were found for histone modification targets of these miRNAs. Several relevant pathways, such as estrogen receptor (ESR)-mediated signalling, estrogen-dependent gene expression, reproduction and oxidative stress induced senescence, showed high levels of enrichment.

We observed that *hsa-miR-223*, *hsa-miR-let-7a* and *miR-145* were highly expressed in the no-labour and low in the labour group. *hsa-miR145* was at the top of the significantly differentially expressed list with more than 4-fold down-regulation in labour samples as compared to the no-labour group. *hsa-miR145* was found to be negatively correlated with ESR1 expression, and several other coding genes. In breast cancer, *hsa-miR-145* has been confirmed to be involved in proapoptotic activities in collaboration with TP53 and represses expression of ESR- α by directly binding to its 3'UTR (Spizzo et al., 2010). The data also included two other miRNAs (*hsa-miR-181a-d* and *hsa-miR-222*) known to be involved in ESR1 pathways (Mou et al., 2017). *miR-181a* and *hsa-miR-222* were low in the no-labour and high in the labour groups. Previously, *miR-181a*, *hsa-miR_23a* and *hsa-miR-26b* were also shown to directly regulate progesterone receptors (Gilan et al., 2017). The data also include four miRNA (*hsa-let-7a-1*, *hsa-let-7f-1*, *hsa-mir-223* and *hsa-mir-29a*) that are known targets of NFkB

(Kumar et al., 2014; Liu et al., 2015b). Among the other differentially changed miRNA, *hsa-miR-132* and *hsa-miR-133* are known to regulate estradiol synthesis (Dai et al., 2013; Li et al., 2015; Wu et al., 2015); *hsa-miR-223*, *hsa-miR-132*, *hsa-miR-199a* and *hsa-miR-31* have a regulatory role in chromatin remodelling (Aprelikova et al., 2010; Alvarez-Saavedra et al., 2011; Sakurai et al., 2011; Zardo et al., 2012; Pagano et al., 2013). Additionally, *hsa-miR-222*, *hsa-miR-141*, *hsa-miR-146*, *hsa-miR-146a*, *hsa-miR-214*, *hsa-miR-33a* and *hsa-miR-411* regulate oxidative stress (Wommack et al., 2018). We performed a correlation analysis between these 27 miRNAs and their 5235 identified mRNA targets. Out of these correlated miRNA:mRNA pairs 48.95% were negative correlations, of which 11.95% were statistically significant (adj. P-value < 0.01; Supplementary Table SIV).

A pathway enrichment of Kyoto Encyclopedia of Genes and Genomes (KEGG) biological network of miRNA:mRNA targets (Pearson correlation > 0.8 and adj. P-value < 0.05) from our RNAseq data is also drawn in Supplementary Fig. S4. Genes in these networks are enriched for NFkB signalling, innate immune and cytokine pathways. Protein domain analysis showed enrichment for histone (H4/H2B) and zinc-binding domains, SNT, Cullin and RNA-binding domains, as confirmed with SMART (Letunic et al., 2021) and InterPro database (Blum et al., 2021) analysis. These proteins were enriched for splicing and RNA transport gene ontologies.

Table 1 Transcription factor enrichment in promoter regions, 1000 bp upstream and 5000 bp downstream of transcription start site.

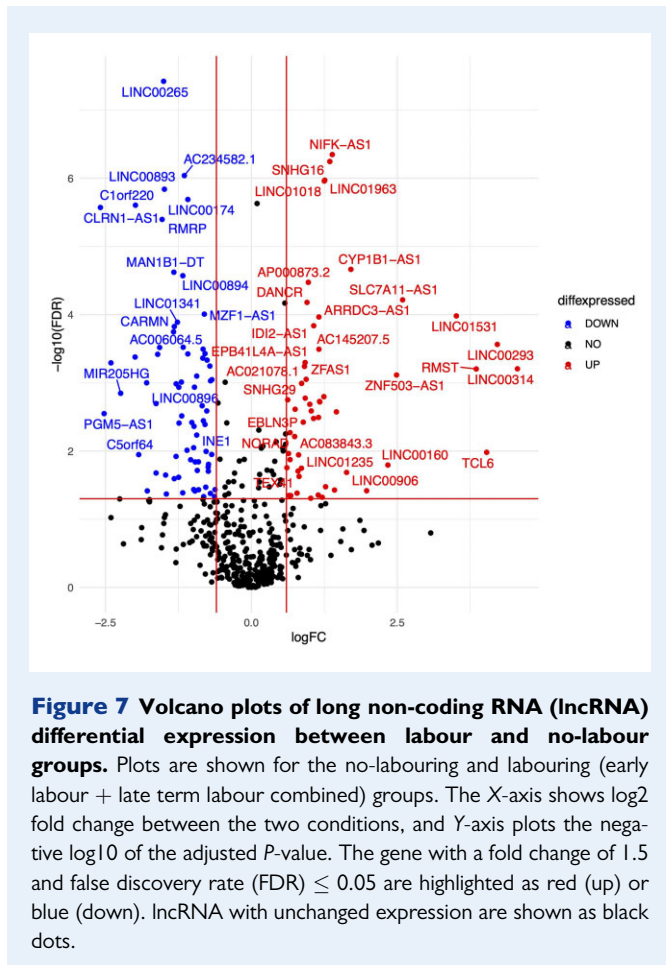
Module	Transcription factor	JASPAR ID	Family	Z-score
M1	Klf4	MA0039.2	BetaBetaAlpha-zinc finger	19.788
	ELF5	MA0136.1	Ets	14.911
	SPIB	MA0081.1	Ets	14.88
	NFATC2	MA0152.1	Rel	14.189
	CTCF	MA0139.1	BetaBetaAlpha-zinc finger	14.041
	RREB1	MA0073.1	BetaBetaAlpha-zinc finger	12.698
	Egr1	MA0162.1	BetaBetaAlpha-zinc finger	12.294
	API	MA0099.2	Leucine Zipper	11.918
	SPI	MA0079.2	BetaBetaAlpha-zinc finger	11.897
	REL	MA0101.1	Rel	11.878
	FEV	MA0156.1	Ets	10.903
	RUNX1	MA0002.2	Runt	10.883
	SPII	MA0080.2	Ets	10.316
	SRF	MA0083.1	MADS	10.171
M2	SRF	MA0083.1	MADS	33.716
	ELF5	MA0136.1	Ets	25.815
	SPIB	MA0081.1	Ets	25.182
	RUNX1	MA0002.2	Runt	21.96
	TEAD1	MA0090.1	Homeo	16.75
	PPARG::RXRA	MA0065.2	Hormone-nuclear Receptor	16.15
	NFATC2	MA0152.1	Rel	15.48
	Hand1::Tcf2a	MA0092.1	Helix-Loop-Helix	15.36
	REL	MA0101.1	Rel	14.84
	FEV	MA0156.1	Ets	14.80
	Foxa2	MA0047.2	Winged Helix-Turn-Helix	14.77
	TBP	MA0108.2	Beta-sheet	14.08
	MEF2A	MA0052.1	Other Alpha-Helix	14.03
	Klf4	MA0039.2	Zinc-coordinating	13.55
	SOX9	MA0077.1	Other Alpha-Helix	12.92
	MEF2A	MA0052.1	MADS	12.85
	API	MA0099.2	Leucine Zipper	12.75
	HOXA5	MA0158.1	Homeo	11.96
MYB	MA0100.1	Myb	11.86	
M3	STAT1	MA0137.2	Stat	22.02
	Gata1	MA0035.2	GATA	17.58
	NF-kappaB	MA0061.1	Rel	17.53
	RELA	MA0107.1	Rel	17.25
	CTCF	MA0139.1	BetaBetaAlpha-zinc finger	16.78
	FEV	MA0156.1	Ets	11.24
	FOXJ1	MA0042.1	Forkhead	10.51

Over-representation of transcription factor binding sites from the JASPAR database was analysed. The top results were ranked by Z-score at a cut-off of Z-score = 10.

lncRNA expression profiling

In the differential expression analysis of the transcriptome, we identified 146 differentially changed lncRNA ($FDR \leq 0.05$) that are known targets of miRNA differentially expressed in our analysis (Fig. 7). Of these, two lncRNA (AK054607 or SOCS2-AS1, and

LINC00312) have previously been reported in spontaneous labour transcript profiles (Romero et al., 2014). When compared with the background set of lncRNA, mean expression of these lncRNAs at term was found to be higher than expected by chance in all groups.



Further, we looked at the distribution of the altered lncRNAs with respect to various genomic features. We observed that the majority of the lncRNA were in antisense and divergent orientation relative to their nearest coding genes, and these lncRNAs are preferentially distributed around their closest coding genes (Supplementary Fig. S5). Eighty-three of these lncRNAs have been previously reported in association with disease in the databases lncRNA disease (Chen and Yan, 2013), lnc2cancer (Ning et al., 2016) and CLC (Carlevaro-Fita et al., 2017). Another general observation was that their spliced length was longer, and conservation in 20 mammals was higher than expected (data not shown). More investigation would be required to assess whether these properties have functional consequences.

The distribution of these lncRNA suggests that they may be acting as co-regulators to the closely co-located protein-coding genes. These associations can be either positive or negative resulting in enhanced expression or repression of the adjacent protein-coding gene. To test the co-differential expression of mRNA and lncRNA, a correlation analysis between lncRNA:mRNA, and lncRNA:miRNA was performed. There were 2602 mRNA as common targets for both miRNA and lncRNA with a significant negative correlation between miRNA:lncRNA (adj. P-value < 0.01; Supplementary Table SIV and

Fig. S4). The gene ontology suggested that these common targets are involved in RNA processing, splicing, oxidative stress and epigenetic gene regulation processes.

Integrated pathway analysis reveals a combinatorial regulatory network of genes, TFs and ncRNA

We used genes from the three co-expressed modules, their identified TFs, differentially expressed miRNA and their lncRNA targets to perform integrative pathway analysis.

The nodes represent an mRNA (yellow), miRNA (blue), lncRNA (red) or a TF (pink), and the nodes are ranked by their degree and betweenness (Fig. 8). Degree denotes the number of edges connected to a node, while betweenness is a measure of how central a node is in the network. Nodes with high betweenness essentially serve as bridges between different portions of the network i.e. interactions must pass through this node to reach other portions of the network.

Fifteen lncRNA (MCM3AP-AS1, TUG1, MIR29B2CHG, HCG18, LINC00963, KCNQ1OT1, NEAT1, HELLPAR, SNHG16, NUTM2B-AS1, MALAT1, PSMA3-AS1, GABPB1-AS1, NORAD and NKILA), and three TFs (ESR1, RELA and NFkB1) showed high degree (≥ 50), and hence acted as hubs in the network. The following 15 TFs were the most highly overrepresented: NFkB1, SPI, RELA, ESR1, STAT1, E2F1, RUNX1, REL, IRF1, SRF, ESR2, NFE2L2, ELK1, SPII and FOXO3.

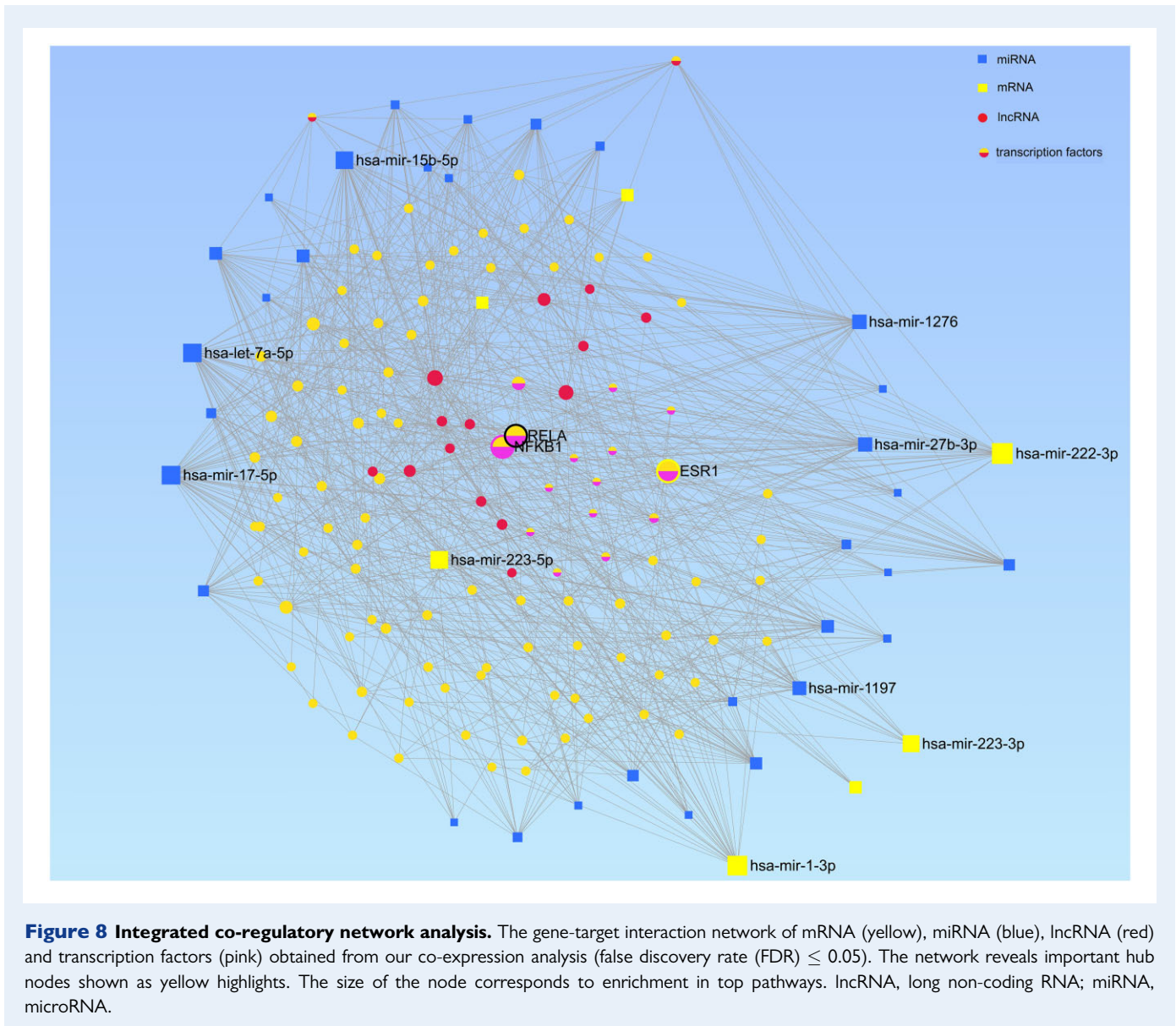
From our list of 27 differentially expressed miRNA, 21 showed high degree (> 10) in the network (*hsa-let-7a*, *hsa-let-7f*, *hsa-mir-1*, *hsa-mir-1197*, *hsa-mir-1276*, *hsa-mir-145*, *hsa-mir-151a*, *hsa-mir-15b*, *hsa-mir-17*, *hsa-mir-181a*, *hsa-mir-222*, *hsa-mir-223*, *hsa-mir-23b*, *hsa-mir-27b*, *hsa-mir-29a*, *hsa-mir-3150b*, *hsa-mir-378a*, *hsa-mir-3975*, *hsa-mir-4768*, *hsa-mir-5690* and *hsa-mir-873*). These miRNAs appear to be regulated by the previously mentioned 15 different TFs (Supplementary Table SIII).

Discussion

Understanding complex interactions between different functional genomic factors driving a phenotype requires integrated analysis of high-throughput genomics datasets. Here, we provide a workflow combining existing and new omics data to dissect the role of different omics layers in regulating term labour. Our approach provides a holistic view of the genome architecture and combinatorial interactions within the various functional layers that bring about changes in the muscle of the uterus at term labour (Fig. 1).

To the best of our knowledge, no previous RNAseq studies have sequenced the whole transcriptome of myometrium at the ultra-deep level (> 100 million reads/sample). We obtained co-expressed gene modules and ncRNA expression profiles associated with non-labouring and labouring groups. We also identified evidence for the active enhancer-promoter pairs and the TFs that directly regulate the gene modules corresponding to labouring and non-labouring groups.

A number of lncRNA changed significantly in term labour samples (Ramírez-Colmenero et al., 2020). We discuss, as an example, lncRNA NKILA that is known to directly interact with and inhibit NFkB pathways by binding to P65 (Liu et al., 2015a; Huang et al., 2016, 2018). It has been shown previously that placental production



of corticotropin-releasing hormone (CRH) is linked to gestational length in human, with a more rapid increase in CRH linked to preterm birth (McLean et al., 1995; Smith, 2015). CRH is also linked to the exponential rise in maternal oestriol in late pregnancy (Ellis et al., 2002), and oestriol dominance over estradiol to the onset of preterm and term labour (Smith et al., 2013, 2009). CRH has also been shown to stimulate the NF κ B system, which can initiate labour (Zbytek et al., 2004). There is strong evidence that estrogens and NF κ B are key components in the onset of labour. Progesterone withdrawal during labour up-regulates ESR1 and allows estrogen action (Mesiano et al., 2002). The ESRs can activate target genes either through direct binding to an estrogen-responsive element in the target gene promoter, or indirectly through interaction with another DNA-binding protein such as NF κ B. We found the expression of lnc species NKILA down from control to the early labour group and up again in the late labour. This

is consistent with NKILA preventing the onset of labour by suppression of NF κ B pathways during pregnancy but a fall of NKILA allowing the onset and progression of labour via NF κ B activation. Integrative analysis revealed 14 new lncRNAs as hub genes in a combinatorial regulatory network. Our data indicate that the lncRNA target their nearest coding genes in a sense-antisense manner.

There is a small but growing body of research that suggests that miRNA can be involved in regulating molecular mechanisms underpinning uterine muscle contraction during term labour (Elovitz et al., 2014; Ackerman et al., 2018; Cook et al., 2019). miRNA activity can be impacted by interactions with other molecules. For example, the 'sponge effect' refers to an interaction of miRNA with lncRNA. The lncRNA usually has a fully complementary sequence that matches a given miRNA and is thus able to bind to that miRNA, preventing it from inhibiting mRNA translation. An lncRNA that acts in this manner

has been named as a competing endogenous RNA (Salmena *et al.*, 2011). We provide evidence that miRNA and lncRNA work synergistically in the form of complex networks to regulate expression of their target genes in term labour. We selected lncRNA:miRNA pairs that have previously been confirmed by CLIP-Seq (Hafner *et al.*, 2021) captures.

The integrative network analysis showed key enriched pathways regulated by ESR1, NFkB, RELA and SPI TFs. Our data showed that these ncRNAs and TFs are involved in regulating estrogen action, oxidative stress, histone modification and chromatin modelling. These network signals are therefore strongly associated with pathways that bring about changes in genome conformation resulting in cascading transcriptional changes leading to the labour phenotype.

Our analysis of TFBS in the promoter and active enhancers identifies TFs responsible for driving module-specific co-regulation. As a result, we report three groups of TFs regulating co-expression of the smooth muscle phenotype in M2, and those driving transcription of modules enriched in labour specific modules M1 and M3. As expected, binding sites for TFs RELA, NFkB and ESR1 were found overrepresented in the regulatory regions of M1 and M3 genes only, and not for the M2 genes.

Conclusion

Collectively, our results demonstrate the epigenomic signatures, and transcriptional responses associated with a term labour phenotype. We identified key components of a likely complex regulatory network that works through combinatorial interactions to drive these changes. Pregnancy hormones at term will induce a cascade of signalling pathways that will in turn affect chromatin conformation, thereby exposing regulating elements, and biomolecule interactions to carry out large-scale transcriptional changes within TADs; as a result the myometrium changes from a relaxed to a contractile phenotype.

Ultra-deep sequencing of the whole transcriptome made it possible to gain a global profile of the term labour transcriptome at high resolution. ncRNAs vary hugely in their size and abundance and analysing short and long ncRNA together increased the sensitivity of analysis. The abundance of differentially expressed ncRNAs necessitated a targeted analysis of different classes of ncRNA. Further, our gene profile signatures along with existing genome-wide chromatin capture data indicate that the 3-dimensional structure of the genome can determine the formation of specific transcriptional units. Our work informs future chromatin conformation captures from term non-labour and labour cohorts to dissect corresponding chromatin domains and subdomains.

Overall, we demonstrate the power of integrated analysis to obtain a holistic view of the term labour phenotype. Such approaches will expedite discovery of robust and reproducible treatments for pregnancy complications related to labour, such as preterm birth, dystocia and postpartum haemorrhage.

Supplementary data

Supplementary data are available at *Molecular Human Reproduction* online.

Data availability

The authors confirm that all relevant data are included in the paper and/or its [supplementary information](#) files. Raw and some processed data have been uploaded to Gene Expression Omnibus (GEO) under the project ID GSE186763.

Acknowledgements

S.T. would like to thank Tyrone Chen, David MacPherson and Rithika Venkatesan from the Tyagi Lab for their help in data curation from public databases and visualization.

Authors' roles

Conceptualization, S.T., R.S. and E.-C.C.; methodology, S.T. and E.C.C.; formal analysis, S.T., E.S.; D.B., P.M., K.A.T.; resources, R.S. and S.T.; data curation, R.S. and S.T.; writing—original draft preparation, S.T.; writing—review and editing, R.S. and S.T.; visualization, S.T. and E.S.; supervision, R.S.; project administration, R.S.; funding acquisition, R.S. and S.T. All authors have read and agreed to the published version of the manuscript.

Funding

S.T. and R.S. acknowledge National Health and Medical Research Council (NHMRC) funding (APPI126795). S.T. acknowledges the AISRF EMCR Fellowship by the Australian Academy of Science, and Australian Women Research Success Grant (AWRSG 2020/2021) by Monash University.

Conflict of interest

The authors declare no competing interests.

References

- Ackerman WE 4th, Buhimschi IA, Brubaker D, Maxwell S, Rood KM, Chance MR, Jing H, Mesiano S, Buhimschi CS. Integrated microRNA and mRNA network analysis of the human myometrial transcriptome in the transition from quiescence to labor. *Biol Reprod* 2018;**98**:834–845.
- Alvarez-Saavedra M, Antoun G, Yanagiya A, Oliva-Hernandez R, Cornejo-Palma D, Perez-Iratxeta C, Sonenberg N, Cheng H-YM. miRNA-132 orchestrates chromatin remodeling and translational control of the circadian clock. *Hum Mol Genet* 2011;**20**:731–751.
- Aprelikova O, Yu X, Palla J, Wei B-R, John S, Yi M, Stephens R, Simpson RM, Risinger JI, Jazaeri A *et al.* The role of miR-31 and its target gene SATB2 in cancer-associated fibroblasts. *Cell Cycle* 2010;**9**:4387–4398.
- Bethin KE, Nagai Y, Sladek R, Asada M, Sadovsky Y, Hudson TJ, Muglia LJ. Microarray analysis of uterine gene expression in mouse and human pregnancy. *Mol Endocrinol* 2003;**17**:1454–1469.

- Blum M, Chang H-Y, Chuguransky S, Grego T, Kandasaamy S, Mitchell A, Nuka G, Paysan-Lafosse T, Qureshi M, Raj S et al. The InterPro protein families and domains database: 20 years on. *Nucleic Acids Res* 2021;**49**:D344–D354.
- Bonev B, Cavalli G. Erratum: organization and function of the 3D genome. *Nat Rev Genet* 2016;**17**:772.
- Bukowski R, Hankins GDV, Saade GR, Anderson GD, Thornton S. Labor-associated gene expression in the human uterine fundus, lower segment, and cervix. *PLoS Med* 2006;**3**:e169.
- Carlevaro-Fita J, Liu L, Zhou Y, Zhang S, Chouvardas P, Johnson R, Li J. LnCompare: gene set feature analysis for human long non-coding RNAs. *Nucleic Acids Res* 2019;**47**:W523–W529.
- Carlevaro-Fita J, Lanzós A, Feuerbach L, Hong C, Mas-Ponte D, Pedersen JS, PCAWG Drivers and Functional Interpretation Group, Johnson J, PCAWG Consortium. Cancer LncRNA Census reveals evidence for deep functional conservation of long noncoding RNAs in tumorigenesis. *Commun Biol* 2020;**3**:56.
- Chan EC, Fraser S, Yin S, Yeo G, Kwek K, Fairclough RJ, Smith R. Human myometrial genes are differentially expressed in labor: a suppression subtractive hybridization study. *J Clin Endocrinol Metab* 2002;**87**:2435–2441.
- Chang L, Zhou G, Soufan O, Xia J. miRNet 2.0: network-based visual analytics for miRNA functional analysis and systems biology. *Nucleic Acids Res* 2020;**48**:W244–W251.
- Chen X, Yan G-Y. Novel human lncRNA–disease association inference based on lncRNA expression profiles. *Bioinformatics* 2013;**29**:2617–2624.
- Cook J, Bennett PR, Kim SH, Teoh TG, Sykes L, Kindinger KM, Garrett A, Binkhamis R, MacIntyre DA, Terzidou V. First trimester circulating microRNA biomarkers predictive of subsequent preterm delivery and cervical shortening. *Sci Rep* 2019;**9**:5861.
- Dai A, Sun H, Fang T, Zhang Q, Wu S, Jiang Y, Ding L, Yan G, Hu Y. MicroRNA-133b stimulates ovarian estradiol synthesis by targeting Foxl2. *FEBS Lett* 2013;**587**:2474–2482.
- Dixon JR, Jung I, Selvaraj S, Shen Y, Antosiewicz-Bourget JE, Lee AY, Ye Z, Kim A, Rajagopal N, Xie W et al. Chromatin architecture reorganization during stem cell differentiation. *Nature* 2015;**518**:331–336.
- Dixon JR, Selvaraj S, Yue F, Kim A, Li Y, Shen Y, Hu M, Liu JS, Ren B. Topological domains in mammalian genomes identified by analysis of chromatin interactions. *Nature* 2012;**485**:376–380.
- Ellis MJ, Livesey JH, Inder WJ, Prickett TCR, Reid R. Plasma corticotropin-releasing hormone and unconjugated estriol in human pregnancy: gestational patterns and ability to predict preterm delivery. *Am J Obstet Gynecol* 2002;**186**:94–99.
- Elovitz MA, Brown AG, Anton L, Gilstrap M, Heiser L, Bastek J. Distinct cervical microRNA profiles are present in women destined to have a preterm birth. *Am J Obstet Gynecol* 2014;**210**:e1–11.
- Esplin MS, Fausett MB, Peltier MR, Hamblin S, Silver RM, Branch DW, Adashi EY, Whiting D. The use of cDNA microarray to identify differentially expressed labor-associated genes within the human myometrium during labor. *Am J Obstet Gynecol* 2005;**193**:404–413.
- Franke M, Ibrahim DM, Andrey G, Schwarzer W, Heinrich V, Schöpflin R, Kraft K, Kempfer R, Jerković I, Chan W-L et al. Formation of new chromatin domains determines pathogenicity of genomic duplications. *Nature* 2016;**538**:265–269.
- Frankish A, Diekhans M, Ferreira A-M, Johnson R, Jungreis I, Loveland J, Mudge JM, Sisu C, Wright J, Armstrong J et al. GENCODE reference annotation for the human and mouse genomes. *Nucleic Acids Res* 2019;**47**:D766–D773.
- Gao T, Qian J. EnhancerAtlas 2.0: an updated resource with enhancer annotation in 586 tissue/cell types across nine species. *Nucleic Acids Res* 2020;**48**:D58–D64.
- Gearing LJ, Cumming HE, Chapman R, Finkel AM, Woodhouse IB, Luu K, Gould JA, Forster SC, Hertzog PJ. CiiiDER: a tool for predicting and analysing transcription factor binding sites. *PLoS One* 2019;**14**:e0215495.
- Gilam A, Shai A, Ashkenazi I, Sarid LA, Drobot A, Bickel A, Shomron N. MicroRNA regulation of progesterone receptor in breast cancer. *Oncotarget* 2017;**8**:25963–25976.
- Hafner M, Katsantoni M, Köster T, Marks J, Mukherjee J, Staiger D, Ule J, Zavolan M. CLIP and complementary methods. *Nat Rev Methods Primers* 2021;**1**:1–23.
- Hanley GE, Munro S, Greyson D, Gross MM, Hundley V, Spiby H, Janssen PA. Diagnosing onset of labor: a systematic review of definitions in the research literature. *BMC Pregnancy Childbirth* 2016;**16**:71.
- Hou C, Li L, Qin ZS, Corces VG. Gene density, transcription, and insulators contribute to the partition of the Drosophila genome into physical domains. *Mol Cell* 2012;**48**:471–484.
- Huang D, Chen J, Yang L, Ouyang Q, Li J, Lao L, Zhao J, Liu J, Lu Y, Xing Y et al. NKILA lncRNA promotes tumor immune evasion by sensitizing T cells to activation-induced cell death. *Nat Immunol* 2018;**19**:1112–1125.
- Huang W, Cui X, Chen J, Feng Y, Song E, Li J, Liu Y. Long non-coding RNA NKILA inhibits migration and invasion of tongue squamous cell carcinoma cells via suppressing epithelial-mesenchymal transition. *Oncotarget* 2016;**7**:62520–62532.
- Keelan JA, Blumenstein M, Helliwell RJA, Sato TA, Marvin KW, Mitchell MD. Cytokines, Prostaglandins and parturition—a review. *Placenta* 2003;**24**:S33–S46.
- Khan A, Fornes O, Stigliani A, Gheorghe M, Castro-Mondragon JA, van der Lee R, Bessy A, Chèneby J, Kulkarni SR, Tan G et al. JASPAR 2018: update of the open-access database of transcription factor binding profiles and its web framework. *Nucleic Acids Res* 2018;**46**:D1284.
- Kim D, Paggi JM, Park C, Bennett C, Salzberg SL. Graph-based genome alignment and genotyping with HISAT2 and HISAT-genotype. *Nat Biotechnol* 2019;**37**:907–915.
- Kota SK, Gayatri K, Jammula S, Kota SK, Krishna SVS, Meher LK, Modi KD. Endocrinology of parturition. *Indian J Endocrinol Metab* 2013;**17**:50–59.
- Kozomara A, Birgaoanu M, Griffiths-Jones S. miRBase: from microRNA sequences to function. *Nucleic Acids Res* 2019;**47**:D155–D162.
- Kumar V, Palermo R, Talora C, Campese AF, Checquolo S, Bellavia D, Tottone L, Testa G, Miele E, Indraco S et al. Notch and NF- κ B signaling pathways regulate miR-223/FBXW7 axis in T-cell acute lymphoblastic leukemia. *Leukemia* 2014;**28**:2324–2335.
- Kwon AT, Arenillas DJ, Worsley Hunt R, Wasserman WW. oPOSSUM-3: advanced analysis of regulatory motif overrepresentation across genes or ChIP-Seq datasets. *G3 (Bethesda)* 2012;**2**:987–1002.

- Law CW, Chen Y, Shi W, Smyth GK. voom: precision weights unlock linear model analysis tools for RNA-seq read counts. *Genome Biol* 2014;**15**:R29.
- Letunic I, Khedkar S, Bork P. SMART: recent updates, new developments and status in 2020. *Nucleic Acids Res* 2021;**49**:D458–D460.
- Liang M, Soomro A, Tasneem S, Abatti LE, Alizada A, Yuan X, Uusküla-Reimand L, Antounians L, Alvi SA, Paterson AD et al. Enhancer-gene rewiring in the pathogenesis of Quebec platelet disorder. *Blood* 2020;**136**:2679–2690.
- Liao Y, Smyth GK, Shi W. featureCounts: an efficient general purpose program for assigning sequence reads to genomic features. *Bioinformatics* 2014;**30**:923–930.
- Liao Y, Smyth GK, Shi W. The R package Rsubread is easier, faster, cheaper and better for alignment and quantification of RNA sequencing reads. *Nucleic Acids Res* 2019;**47**:e47.
- Lieberman-Aiden E, van Berkum NL, Williams L, Imakaev M, Ragoczy T, Telling A, Amit I, Lajoie BR, Sabo PJ, Dorschner MO et al. Comprehensive mapping of long-range interactions reveals folding principles of the human genome. *Science* 2009;**326**:289–293.
- Lin Y, Liu T, Cui T, Wang Z, Zhang Y, Tan P, Huang Y, Yu J, Wang D. RNAInter in 2020: RNA interactome repository with increased coverage and annotation. *Nucleic Acids Res* 2020;**48**:D189–D197.
- Liu B, Sun L, Liu Q, Gong C, Yao Y, Lv X, Lin L, Yao H, Su F, Li D et al. A cytoplasmic NF- κ B interacting long noncoding RNA blocks I κ B phosphorylation and suppresses breast cancer metastasis. *Cancer Cell* 2015a;**27**:370–381.
- Liu J, Zhu L, Xie G-L, Bao J-F, Yu Q. Let-7 miRNAs modulate the activation of NF- κ B by targeting TNFAIP3 and are involved in the pathogenesis of lupus nephritis. *PLoS One* 2015b;**10**:e0121256.
- Li Y, Fang Y, Liu Y, Yang X. MicroRNAs in ovarian function and disorders. *J Ovarian Res* 2015;**8**:51.
- Lui S, Duval C, Farrokhnia F, Girard S, Harris LK, Tower CL, Stevens A, Jones RL. Delineating differential regulatory signatures of the human transcriptome in the choriondecidua and myometrium at term labor. *Biol Reprod* 2018;**98**:422–436.
- Lupiáñez DG, Kraft K, Heinrich V, Krawitz P, Brancati F, Klopocki E, Horn D, Kayserili H, Opitz JM, Laxova R et al. Disruptions of topological chromatin domains cause pathogenic rewiring of gene-enhancer interactions. *Cell* 2015;**161**:1012–1025.
- McLean M, Bisits A, Davies J, Woods R, Lowry P, Smith R. A placental clock controlling the length of human pregnancy. *Nat Med* 1995;**1**:460–463.
- Merienne N, Meunier C, Schneider A, Seguin J, Nair SS, Rocher AB, Le Gras S, Keime C, Faull R, Pellerin L et al. Cell-type-specific gene expression profiling in adult mouse brain reveals normal and disease-state signatures. *Cell Rep* 2019;**26**:2477–2493.e9.
- Mesiano S, Chan E-C, Fitter JT, Kwek K, Yeo G, Smith R. Progesterone withdrawal and estrogen activation in human parturition are coordinated by progesterone receptor A expression in the myometrium. *J Clin Endocrinol Metab* 2002;**87**:2924–2930.
- Mittal P, Romero R, Tarca AL, Gonzalez J, Draghici S, Xu Y, Dong Z, Nhan-Chang C-L, Chaiworapongsa T, Lye S et al. Characterization of the myometrial transcriptome and biological pathways of spontaneous human labor at term. *J Perinat Med* 2010;**38**:617–643.
- Mootha VK, Lindgren CM, Eriksson K-F, Subramanian A, Sihag S, Lehar J, Puigserver P, Carlsson E, Ridderstråle M, Laurila E et al. PGC-1 α -responsive genes involved in oxidative phosphorylation are coordinately downregulated in human diabetes. *Nat Genet* 2003;**34**:267–273.
- Mou T, Zhu D, Wei X, Li T, Zheng D, Pu J, Guo Z, Wu Z. Identification and interaction analysis of key genes and microRNAs in hepatocellular carcinoma by bioinformatics analysis. *World J Surg Oncol* 2017;**15**:63.
- Muro EM, Ibn-Salem J, Andrade-Navarro MA. The distributions of protein coding genes within chromatin domains in relation to human disease. *Epigenetics Chromatin* 2019;**12**:72.
- Myers KM, Feltovich H, Mazza E, Vink J, Bajka M, Wapner RJ, Hall TJ, House M. The mechanical role of the cervix in pregnancy. *J Biomech* 2015;**48**:1511–1523.
- Narendra V, Rocha PP, An D, Raviram R, Skok JA, Mazzoni EO, Reinberg D. CTCF establishes discrete functional chromatin domains at the Hox clusters during differentiation. *Science* 2015;**347**:1017–1021.
- Ning S, Zhang J, Wang P, Zhi H, Wang J, Liu Y, Gao Y, Guo M, Yue M, Wang L et al. Lnc2Cancer: a manually curated database of experimentally supported lncRNAs associated with various human cancers. *Nucleic Acids Res* 2016;**44**:D980–D985.
- Nora EP, Lajoie BR, Schulz EG, Giorgetti L, Okamoto I, Servant N, Piolot T, van Berkum NL, Meisig J, Sedat J et al. Spatial partitioning of the regulatory landscape of the X-inactivation centre. *Nature* 2012;**485**:381–385.
- Pagano F, De Marinis E, Grignani F, Nervi C. Epigenetic role of miRNAs in normal and leukemic hematopoiesis. *Epigenomics* 2013;**5**:539–552.
- Phillips-Cremins JE, Sauria MEG, Sanyal A, Gerasimova TI, Lajoie BR, Bell JSK, Ong C-T, Hookway TA, Guo C, Sun Y et al. Architectural protein subclasses shape 3D organization of genomes during lineage commitment. *Cell* 2013;**153**:1281–1295.
- Ramírez-Colmenero A, Oktaba K, Fernandez-Valverde SL. Evolution of genome-organizing long non-coding RNAs in metazoans. *Front Genet* 2020;**11**:589697.
- Rao SSP, Huntley MH, Durand NC, Stamenova EK, Bochkov ID, Robinson JT, Sanborn AL, Machol I, Omer AD, Lander ES et al. A 3D map of the human genome at kilobase resolution reveals principles of chromatin looping. *Cell* 2014;**159**:1665–1680.
- Reimand J, Isserlin R, Voisin V, Kucera M, Tannus-Lopes C, Rostamianfar A, Wadi L, Meyer M, Wong J, Xu C et al. Pathway enrichment analysis and visualization of omics data using g:Profiler, GSEA, Cytoscape and EnrichmentMap. *Nat Protoc* 2019;**14**:482–517.
- Robinson MD, McCarthy DJ, Smyth GK. edgeR: a Bioconductor package for differential expression analysis of digital gene expression data. *Bioinformatics* 2010;**26**:139–140.
- Romero R, Tarca AL, Chaemsaitong P, Miranda J, Chaiworapongsa T, Jia H, Hassan SS, Kalita CA, Cai J, Yeo L et al. Transcriptome interrogation of human myometrium identifies differentially expressed sense-antisense pairs of protein-coding and long non-coding RNA genes in spontaneous labor at term. *J Matern Fetal Neonatal Med* 2014;**27**:1397–1408.
- Romero R, Tarca AL, Tromp G. Insights into the physiology of childbirth using transcriptomics. *PLoS Med* 2006;**3**:e276.

- Russo PST, Ferreira GR, Cardozo LE, Bürger MC, Arias-Carrasco R, Maruyama SR, Hirata TDC, Lima DS, Passos FM, Fukutani KF et al. CEMiTool: a Bioconductor package for performing comprehensive modular co-expression analyses. *BMC Bioinformatics* 2018; **19**:56.
- Sakurai K, Furukawa C, Haraguchi T, Inada K-I, Shiogama K, Tagawa T, Fujita S, Ueno Y, Ogata A, Ito M et al. MicroRNAs miR-199a-5p and -3p target the Brm subunit of SWI/SNF to generate a double-negative feedback loop in a variety of human cancers. *Cancer Res* 2011; **71**:1680–1689.
- Salmela L, Polisen L, Tay Y, Kats L, Pandolfi PP. A ceRNA hypothesis: the Rosetta Stone of a hidden RNA language? *Cell* 2011; **146**:353–358.
- Sandelin A, Alkema W, Engström P, Wasserman WW, Lenhard B. JASPAR: an open-access database for eukaryotic transcription factor binding profiles. *Nucleic Acids Res* 2004; **32**:D91–D94.
- Sexton T, Yaffe E, Kenigsberg E, Bantignies F, Leblanc B, Hoichman M, Parrinello H, Tanay A, Cavalli G. Three-dimensional folding and functional organization principles of the Drosophila genome. *Cell* 2012; **148**:458–472.
- Sharp GC, Hutchinson JL, Hibbert N, Freeman TC, Saunders PTK, Norman JE. Transcription analysis of the myometrium of labouring and non-labouring women. *PLoS One* 2016; **11**:e0155413.
- Smith R. Reapplying the uterine brake in preterm labor. *Sci Transl Med* 2015; **7**:319fs51.
- Smith R, Butler T, Chan E-C. Do estrogen receptor variants explain the enigma of human birth? *EBioMedicine* 2019; **39**:25–26.
- Smith R, Paul J, Maiti K, Tolosa J, Madsen G. Recent advances in understanding the endocrinology of human birth. *Trends Endocrinol Metab* 2012; **23**:516–523.
- Smith R, Paul JW, Tolosa JM. Sharpey-Schafer Lecture 2019: from retroviruses to human birth. *Exp Physiol* 2020; **105**:555–561.
- Smith R, Smith JJ, Shen X, Engel PJ, Bowman ME, McGrath SA, Bisits AM, McElduff P, Giles WB, Smith DW et al. Patterns of plasma corticotropin-releasing hormone, progesterone, estradiol, and estradiol change and the onset of human labor. *J Clin Endocrinol Metab* 2009; **94**:2066–2074.
- Smith R, Zakar T, Madsen G. Mammalian labor: variations on a theme by amniota. *Endocrinology* 2013; **154**:584–588.
- Spizzo R, Nicoloso MS, Lupini L, Lu Y, Fogarty J, Rossi S, Zagatti B, Fabbri M, Veronese A, Liu X et al. miR-145 participates with TP53 in a death-promoting regulatory loop and targets estrogen receptor- α in human breast cancer cells. *Cell Death Differ* 2010; **17**:246–254.
- Stanfield Z, Lai PF, Lei K, Johnson MR, Blanks AM, Romero R, Chance MR, Mesiano S, Koyutürk M. Myometrial transcriptional signatures of human parturition. *Front Genet* 2019; **10**:185.
- Subramanian A, Tamayo P, Mootha VK, Mukherjee S, Ebert BL, Gillette MA, Paulovich A, Pomeroy SL, Golub TR, Lander ES et al. Gene set enrichment analysis: a knowledge-based approach for interpreting genome-wide expression profiles. *Proc Natl Acad Sci U S A* 2005; **102**:15545–15550.
- Wommack JC, Trzeciakowski JP, Miranda RC, Stowe RP, Ruiz RJ. Micro RNA clusters in maternal plasma are associated with preterm birth and infant outcomes. *PLoS One* 2018; **13**:e0199029.
- Wu S, Sun H, Zhang Q, Jiang Y, Fang T, Cui I, Yan G, Hu Y. MicroRNA-132 promotes estradiol synthesis in ovarian granulosa cells via translational repression of Nurr1. *Reprod Biol Endocrinol* 2015; **13**:94.
- Yang J-H, Li J-H, Shao P, Zhou H, Chen Y-Q, Qu L-H. starBase: a database for exploring microRNA-mRNA interaction maps from Argonaute CLIP-Seq and Degradome-Seq data. *Nucleic Acids Res* 2011; **39**:D202–D209.
- Zabidi MA, Arnold CD, Scherhuber K, Pagani M, Rath M, Frank O, Stark A. Enhancer-core-promoter specificity separates developmental and housekeeping gene regulation. *Nature* 2015; **518**:556–559.
- Zardo G, Ciolfi A, Vian L, Billi M, Racanicchi S, Grignani F, Nervi C. Transcriptional targeting by microRNA-polycomb complexes: a novel route in cell fate determination. *Cell Cycle* 2012; **11**:3543–3549.
- Zbytek B, Pfeffer LM, Slominski AT. Corticotropin-releasing hormone stimulates NF-kappaB in human epidermal keratinocytes. *J Endocrinol* 2004; **181**:R1–R7.
- Zhang B, Horvath S. A general framework for weighted gene co-expression network analysis. *Stat Appl Genet Mol Biol* 2005; **4**:Article17.